JOURNAL OF MATERIALS SCIENCE 27 (1992) 4024–4034

Interphase behaviour in graphite–thermoplastic monofilament composites

Part I *Monotonic loading*

L. S. SCHADLER‡, C. LAIRD
Department of Materials Science and Engineering, University of Pennsylvania, Philadelphia, PA 19139, USA

J. C. FIGUEROA
E. I. Du Pont de Nemours and Co., Inc. Experimental Station, PO Box 80304, Wilmington, DE 19880-0304, USA

The role of the fibre–matrix interphase in transferring load from the matrix to the fibre in graphite–thermoplastic composites is not well understood. The goal of this work was to alter the interphase of graphite–thermoplastic monofilament composites in a controlled manner by treating the fibre surface, and then correlating fibre surface morphology, fibre surface energy, fibre strength, and matrix properties with interphase behaviour. A monofilament composite system was employed to study the fibre–matrix interphase because fibre–fibre interaction and processing variability are eliminated. A fragmentation method was used to observe the interphase behaviour of the monofilament composites indirectly by measuring the interphase shear stress, a parameter which governs the load transfer from the matrix to the fibre. It was found that the improvement in the ability of the interphase to transfer load from the matrix to the fibre increased with the severity of the treatment and was due primarily to increased micromechanical locking (increased surface roughness). Debonding at the interphase occurred along either the fibre–matrix interphase (in the composites with a tough matrix) or perpendicular to the fibre (in composites with a weaker matrix, and a strong interphase). Thus the matrix properties, by limiting the properties of the composite, strongly influenced the value of improving the interphase properties.

1. Introduction

Continuous fibre-reinforced polymer composites are becoming increasingly important engineering materials. Thermoplastic matrix composites have been developed in recent years to replace thermoset composites for several reasons: thermoplastics can be extrusion-moulded, they can be remelted and remoulded for in-the-field repairs, they are less hygroscopic than most thermosets, and some thermoplastics can maintain their mechanical strength at temperatures as high as 250 °C [1].

In many continuous fibre-reinforced polymer composites the fibre modulus is 100 times that of the matrix, and the fibre is the load-bearing component. Load is transferred from the matrix to the fibre through the interphase, defined as the region beginning at the point in the fibre where the properties differ from that of the bulk fibre, and ending at the point in the matrix where the properties become equal to that of the bulk matrix (Fig. 1). A result of this load-transfer process is that the interphase region has a strong influence on composite properties [2–5]. For example, the toughness of a composite depends on the load transfer [2, 6]. In addition, the interphase region can be a nucleation site for failure [7–9] because of the stress concentrations that develop as a result of the large difference in modulus between the matrix and the fibre and the differences in the coefficients of thermal expansion [10].

A useful model system for studying the interphase is a monofilament composite system because fibre–fibre interaction is eliminated, and the interphase can be carefully controlled to yield reproducible samples. Monofilament composites have been used by many groups to study the monotonic behaviour of the interphase in graphite–thermoset composites [2, 3, 11–13], and by a few groups to study the monotonic behaviour of the interphase in thermoplastic composites [14, 15]. Several techniques have been developed to determine the load transfer at the interphase by estimating the interphase shear stress in fibre fragments loaded axially [16].

Work reported here is a continuation to preliminary observations in graphite–polycarbonate that were reported elsewhere [17]. This report presents a comparative analysis between the graphite–

‡ To whom correspondence should be addressed at IBM T. J. Watson Research Center, PO Box 218, Yorktown Heights, NY 10598, USA.

0022–2461

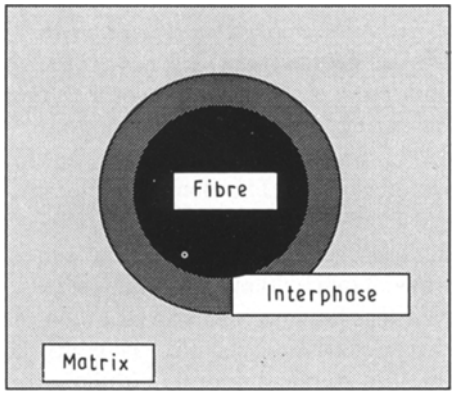

Figure 1 Schematic diagram showing the fibre, matrix, and the interphase region.

polycarbonate and the graphite–nylon systems that explores in further depth the issue of interphase load transfer in monotonically loaded composites. A variation of the critical length technique [18] was used to quantify the effect of changes in fibre surface energy, fibre surface morphology, and fibre tensile strength on the interphase load transfer behaviour. These parameters were altered by plasma-etching the fibres prior to composite fabrication.

2. Experimental procedure

2.1. Materials selection and preparation

Two thermoplastic matrices were chosen for study: polycarbonate and J2®. Polycarbonate was chosen because it is well suited to the fragmentation test; it is a model birefrigent material, with a low T_g for ease of moulding, and has been studied extensively. For comparison J2 (a du Pont de Nemours and Co. Inc. nylon-based material) was studied. The graphite fibre used in this study was AU4 which has a low modulus, and a high strain to failure (170 GPa, 1.5%).

The fibres were cleaned in a bath of Freon 113 for 10 min. The fibre surface was altered with an oxygen plasma-etch to increase the polarity of the surface (improve the chemical interaction), and to remove the outer layers of the fibre and increase the roughness (improve the micromechanical interlocking).

The polycarbonate was cleaned by washing in Freon 113. To eliminate any ageing by water [19] during moulding, the polycarbonate was dried for at least 8 h before moulding.

The monofilament composites were prepared in a mould by placing cleaned and treated fibres, secured at each end, between two sheets of cleaned and dried polycarbonate 150 mm long by 100 mm wide by 0.25 mm thick. The mould was heated to 190 °C between two platens with a pressure of 3900 Pa. The mould was heated at a rate of 3 °C min^{-1} and was air-cooled. Several filaments were placed in each mould.

2.2. Surface energy measurements

The fibre surface energy was determined both before and after various treatments by measuring the contact angles of two liquids on the fibre using a standard

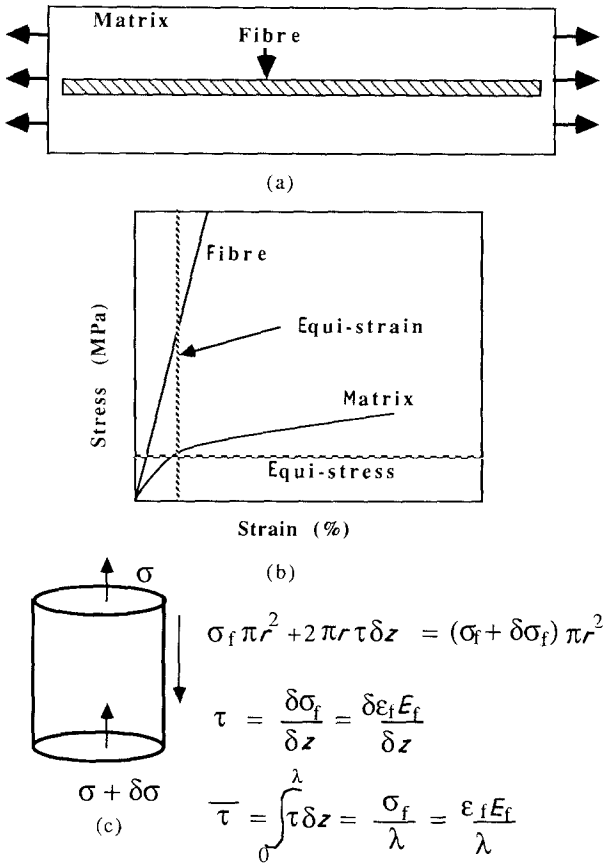

Figure 2 Schematic diagrams showing (a) the geometry of loading a single filament, (b) a stress–strain curve for both the fibre and the matrix in a composite, (c) a force body diagram of a fibre being loaded in tension in a composite. The build-up of load in the fibre is due to shear at the interphase.

Wilhelmy technique [20], and solving the harmonic mean approximation simultaneously for the two liquids [21]. The contact angles were measured at zero velocity. Although the fibre surface treatment employed roughened the surface, the size of the features tended to be small. Because the effect of roughness is negligible for features less than 0.1 μm in size [22], the effect of roughness on the measurement was assumed to be less than the scatter of the data.

2.3. Fragmentation test

Single-filament composite specimens were monotonically deformed along the fibre axis until the fibre fractured at a few places. The photoelastically active stress transfer zones present at the ends of the loaded fibres were measured to estimate an average interphase shear stress (ISS) (Fig. 2a).

If a single-filament composite is deformed in the axial direction, there will be a shear lag between the matrix and the fibre near any fragment ends. The composite will seek an equi-strain condition (Fig. 2b), and as a result load will be transferred from the matrix to the fibre exclusively through an interfacial shear stress. The force equilibrium to describe the load transfer on a section of the fibre is shown schematically in Fig. 2c [23], and mathematically in the equation

$$\sigma_f \pi r_o^2 + 2\pi\tau r_o \delta z = \pi r_o^2(\sigma_f + \delta\sigma_f) \quad (1)$$

where τ is the ISS, z is the distance along the fibre, r_o is the fibre radius and σ_f is the stress in the fibre. This equation can be solved for the shear stress

$$\tau = \left(\frac{\delta\sigma_f}{\delta z}\right)\frac{r_o}{2} = \left(\frac{\delta\varepsilon_f E_f}{\delta Z}\right)\frac{r_o}{2} \quad (2)$$

where ε_f is the strain in the fibre and E_f is the fibre axial modulus. This yields a relationship between the ISS and the build-up of stress in the fibre, but does not solve for either one. The average shear stress within the stress transfer zone of length λ can be obtained from Equation 2 by integrating the shear stress over the length of the stress transfer zone, λ, and dividing by λ

$$\tau = \left(\frac{\sigma_f}{\lambda}\right)\frac{r_o}{2} = \left(\frac{\varepsilon_f E_f}{\lambda}\right)\frac{r_o}{2} \quad (3)$$

The average ISS can be determined experimentally by measuring the length of the stress transfer zone, λ, and the strain in the fibre. We have entitled this method the "lambda technique". The advantage of this technique over convential optical fragmentation techniques is that information about the strength of the fibre is not necessary, eliminating many of the complicated statistics involved with that measurement. λ and the fibre strain were measured using the following method.

The length of the stress transfer zone, λ, was measured by loading a single-filament composite in the axial direction until the fibre began to fail, and by viewing the sample in cross-polarization. In such a test, the stress transfer zone appears as an optically active region surrounding the fibre break. Fig. 3 shows a schematic diagram of what is typically seen in the microscope. The strain in the fibre is assumed to be equal to the strain applied to the composite. However, the strain in the fibre was not measured, and it has been reported that residual axial compressive strain is frozen in during moulding [24]. Therefore, the values presented in this paper are relative average ISS values, not absolute values. The details of the method are presented below.

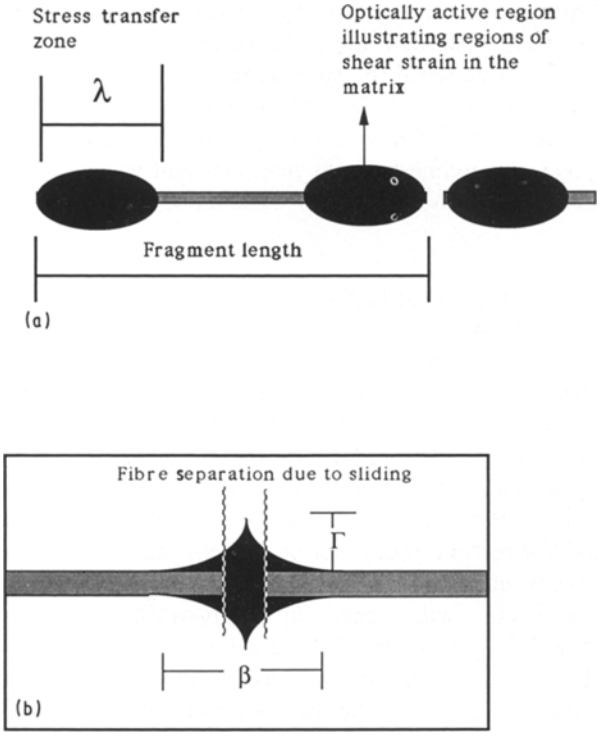

Figure 3 (a) A schematic diagram of what is typically seen in the microscope when a single filament composite is loaded to above the fibre failure strain, and viewed in cross-polarization; (b) a schematic diagram of the crack region surrounding the fibre break.

Single-filament composite tensile samples with dimensions 3 mm × 90 mm × 0.5 mm were cut from the mould. Each composite was mounted on a small screw-driven tensile tester (MTT) controlled by a Compumotor stepping motor with a resolution of 100 μm or better, and equipped with an ultra-miniature load cell (Entran model ELF-500-100). The strain was measured using an MTS extensometer interfaced with a Vishay signal conditioner/amplifier. The load and strain were monitored with a x–y recorder. The entire apparatus was mounted on a Zeiss Axiomat reflection optical microscope with a translating stage. The stage translation was monitored with a linear variable differential transformer (LVDT) with a resolution of 0.5 μm. The test was also recorded with a CCD video camera, and a Sony video cassette recorder. A schematic diagram of the set-up is shown in Fig. 4.

Because the microscope was used in reflection, the composite was placed between a mirror and a glass slide to reflect the optical beam and enhance the image. The polarization and illumination conditions were kept nominally constant for all birefringence measurements. The light source was a metal–halide 250 W short arc lamp, and the aperture was set to the widest opening. The polarizer and the analyser were placed at the angle closest to extinction, and then shifted up to 5°. All measurements were taken at about 100×.

The tests were run at a strain rate of $3.33 \times 10^{-4}\ s^{-1}$. The composites were loaded to an initial strain of 1.4%. The fibre was then scanned for breaks. As the fibre was scanned, the position along the fibre was monitored by the LVDT and recorded with an x–y recorder. At features of interest, such as fibre

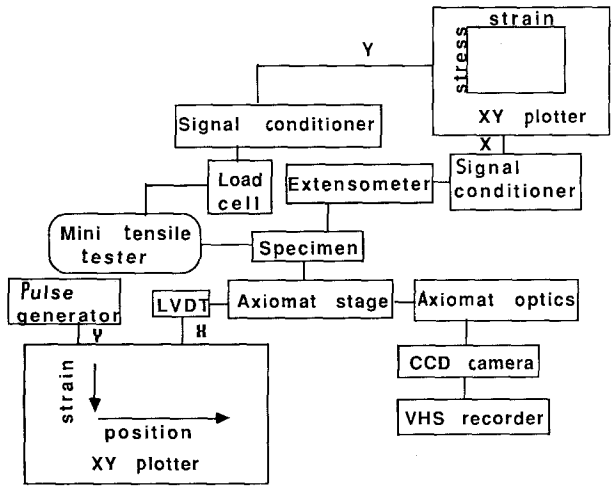

Figure 4 A schematic diagram of the apparatus for the fragmentation test.

breaks, a pulse generator was pulsed to mark the spot. At increments of 0.1% thereafter, the position of fibre breaks was recorded. The test was stopped when no further fragmentation occurred.

After careful analysis, the following error estimates were made. λ was accurate to within $\pm$ 20 μm, the strain to within $\pm$ 0.1% and the fibre radius to within 5%. In addition the ISS values give the average ISS within one transfer zone, averaged over the stress transfer zones for more than 50 fibre breaks, and for several different mouldings.

2.4. Scanning electron microscopy

Scanning electron microscopy (SEM) was used to monitor the surface roughness of the fibres before moulding, and to observe the locus of failure in the interphase region produced by the fragmentation test. All samples were sputtered with gold to eliminate charging effects.

Bare filament samples of AU4 as-received fibres, and fibres that had been plasma-treated from 1–7 min were examined. Fibres that had been embedded in a monofilament composite were viewed by pulling the fibres out of the matrix in two ways. The sample was either notched perpendicular to the fibre direction through the entire thickness of the sample (but not the width of the sample) and pulled to failure, or notched perpendicular to the fibre the entire width of the sample, and bent to failure. In most cases, the fibre pulled out of the matrix to some extent, and could be viewed with the SEM. Samples of AU4 as-received fibres and 1 and 3 min treated fibres in polycarbonate were viewed as well as AU4 as-received and 2 and 7 min treated fibres in J2.

The surface roughness was used to help characterize the surface morphology of the fibre. The surface roughness was determined by measuring the number of protrusions and extrusions in a 4 μm^2 representative area of the fibre at a magnification of 20 000 ×.

3. Results

The results will be presented in the following order: (i) the initial state of the fibre including the fibre surface energy, the fibre surface roughness, and the fibre strength; (ii) parameters from the moulded fibre including the average interphase shear stress (ISS) and photoelastic patterns; and (iii) post-fragmentation test SEM analysis of the fibre surface after pull-out from the matrix.

3.1. Surface morphology, surface energy and fibre strength

The surface treatment alters the fibre surface morphology, which may affect the micromechanical interlocking of the fibre and the matrix. This change in surface morphology was characterized by its roughness. The fibre surface roughness is plotted as a function of fibre surface treatment in Fig. 5a. The roughness increases until 3 min of treatment time,

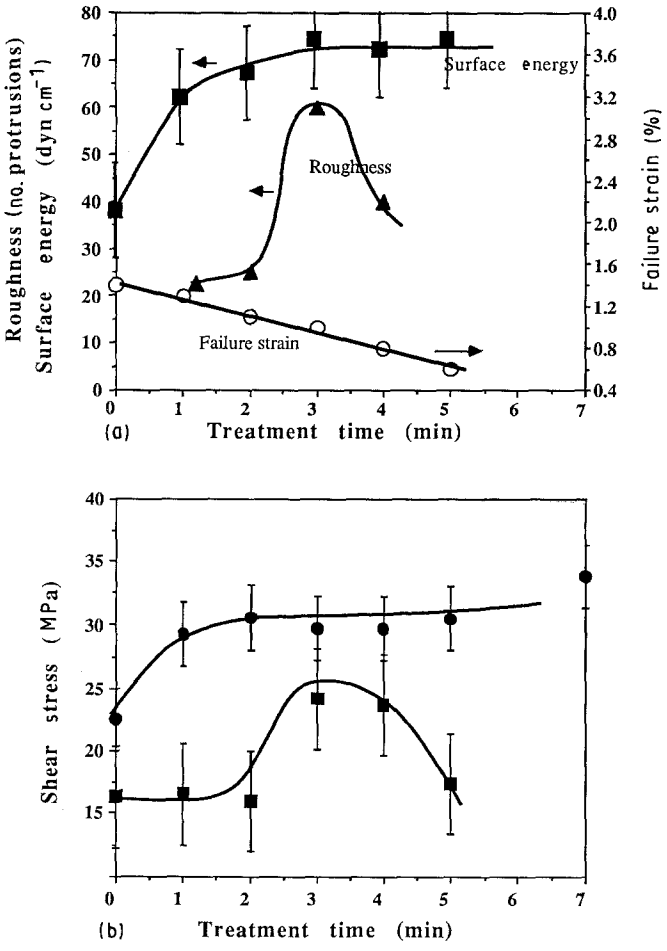

Figure 5 (a) Fibre (▲) roughness, (■) surface energy and (○) failure strain as a function of treatment time; (b) average interphase shear stress as a function of treatment time for (■) polycarbonate and (●) J2. 1 dyn cm^{-1} = 1 mN m^{-1}.

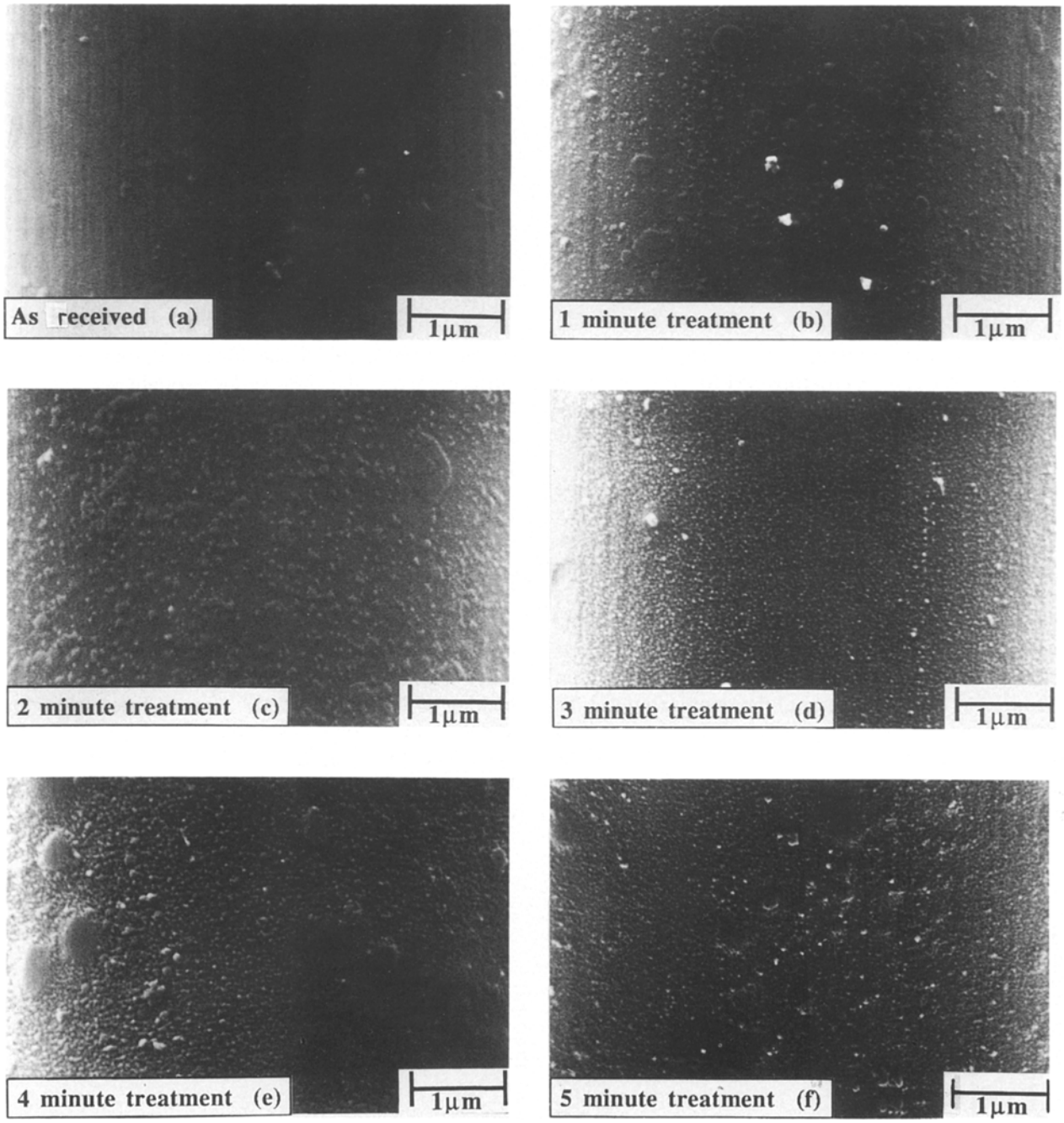

Figure 6 Typical SEM micrographs of AU4 fibres treated for various times: (a) as-received, (b) 1 min, (c) 2 min, (d) 3 min, (e) 4 min, (f) 5 min.

and then decreases. The SEM photographs for fibres treated for 1, 2, 3, 4 and 5 min from which roughness was obtained are shown in Fig. 6.

In addition, the fibre surface treatment alters the surface energy of the fibre which may affect the fibre–matrix bonding as well as the ability of the matrix to wet the fibre. Fig. 5a shows the total fibre surface energy as a function of treatment time, and Fig. 7 shows the breakdown of the total surface energy into the polar and dispersive components. The error bars represent the maximum and minimum values calculated. The surface energy increases rapidly after 1 min of treatment, and then becomes constant.

The fibre tensile strength was determined using sets of monofilament composite specimens and bare fibres [25]. Briefly, fragments lengths, and the strain applied to the composite at the point of fragment failure, were

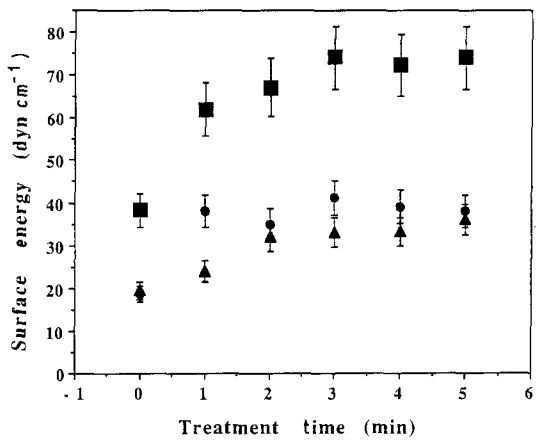

Figure 7 AU4 fibre (■) total surface energy, (●) polar component and (▲) dispersive component as a function of treatment time. 1 dyn cm^{-1} = 1 mN m^{-1}.

correlated for several fibres. Bare fibres were tested using conventional techniques. The tensile strength of the fibre decreased with treatment time as shown in Fig. 5a.

3.2. Interphase shear stress

To measure the effect of the initial state of the fibre on the load transfer behaviour of the interphase, the average ISS was determined using the lambda technique for as-received fibres and fibres treated for 1–7 min for both AU4–PC and AU4–J2 model composites. Fig. 5b presents the average ISS versus treatment time for AU4–PC and AU4–J2. The error bars represent one standard deviation. Each data point for the AU4–J2 composite system represents one sample; each point for the AU4–PC composite system is taken as the average of at least three data points. The average ISS in AU4–PC reaches a maximum after 3 min of treatment, and then decreases; the average ISS in the AU4–J2 composites reaches a plateau after 1 min of treatment.

In addition to the average ISS, the photoelastic patterns were monitored to obtain qualitative information about the shape of the ISS distribution, for as-received fibres, and fibres treated for 1 and 3 min for both composite systems. A pattern for each treatment at several strains is shown in Fig. 7 for the AU4–PC system, and in Fig. 8 for the AU4–J2 system. Optical activity is due to shear stresses in the matrix which develop because of the load transfer from the matrix to the fibre. An absence of optical activity indicates that there is no load transfer. An intense region of optical activity that is oblong in shape represents a region of high matrix shear that varies with distance along the fibre. A long region of low intensity represents a region of low shear stress in the matrix that is constant with distance along the fibre.

In the AU4–PC system, the photoelastic patterns change shape from low applied strain to high applied strain for all three types of fibre. At low strains there is an oblong region of intense light. At higher strains, the region closest to the fibre break is of low intensity, and the oblong region of high intensity has moved along the fibre. This suggests that a crack or a yield zone propagates along the interphase as strain is applied to the fibre, creating a region of constant ISS.The regions of photoelastic activity are shorter for the fibre treated for 3 min than for the as-received fibre, suggesting that the average ISS is greater for the treated fibre even though the overall shape of the patterns is the same.

The photoelastic patterns for the as-received fibres in J2 (Fig. 9) are similar to those in PC. At low strains there is a region of intense optical activity that migrates away from the fibre break with applied strain. However, the length of the region of intense optical activity (stress transfer zone) remains close to the fibre break for fibres treated for 1 and 3 min, and the length of the stress transfer zone remains constant with applied strain. It is difficult to reproduce on film, but a crack forms in the matrix, perpendicular to the fibre in the composites with treated fibres. The cracks are

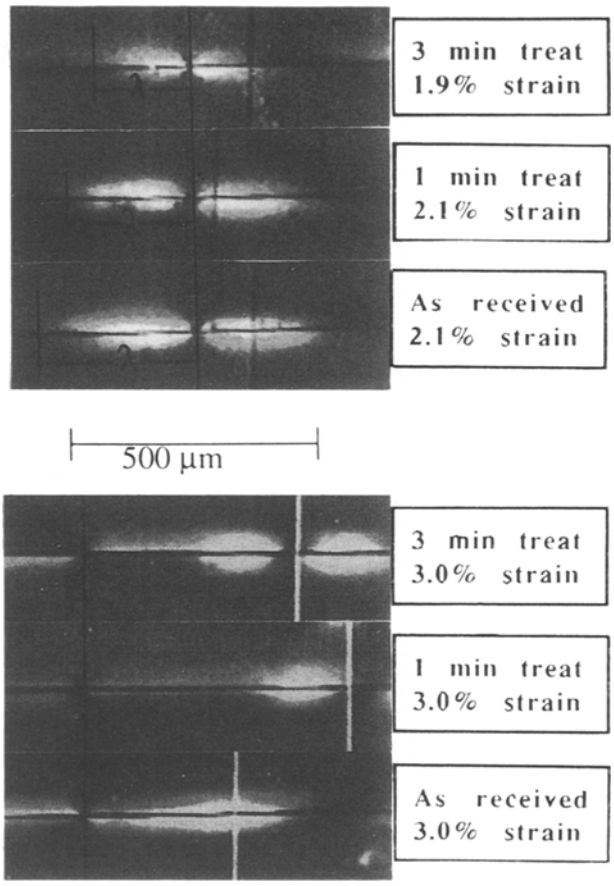

Figure 8 Typical photoelastic patterns in polycarbonate for as-received fibres, and fibres treated for 1 and 3 min at two strain levels: ~ 2.0 and 3.0%.

penny-shaped cracks with a tip-to-tip distance of about 1.6 fibre diameters. However, quantitative measurements of crack length and changes in crack length with treatment time and applied strain were not made. The evidence for the crack is that the width of the optically active zone near the fibre break is wider than the fibre, indicating that there is a crack that is wider than the fibre diameter. The constant length of the stress transfer zone implies that there is no additional load transferred to the fibre. The interpretation is that the matrix crack prevents a crack or a yield zone from propagating along the fibre, and relieves the strain in the fibre. Fig. 3 shows a schematic diagram of the crack region surrounding a break. In J2, $\Gamma > 0$ and $\beta \approx 0$.

3.3. Scanning electron microscopy of fibre surfaces

To determine the locus of failure in the interphase, samples pulled from the matrix were viewed by SEM. The locus of failure produced during the fragmentation test was seen to vary with treatment time for both the AU4–PC and the AU4–J2 composite systems. Fig. 10a–c compare the bare fibre surface for an as-received fibre, a 1 min treated and a 3 min treated fibre, respectively; Fig. 10d–f show the same types of fibre moulded in polycarbonate and pulled from the matrix, while Fig. 10g–i show the same types of fibre moulded in J2 and pulled from the matrix.

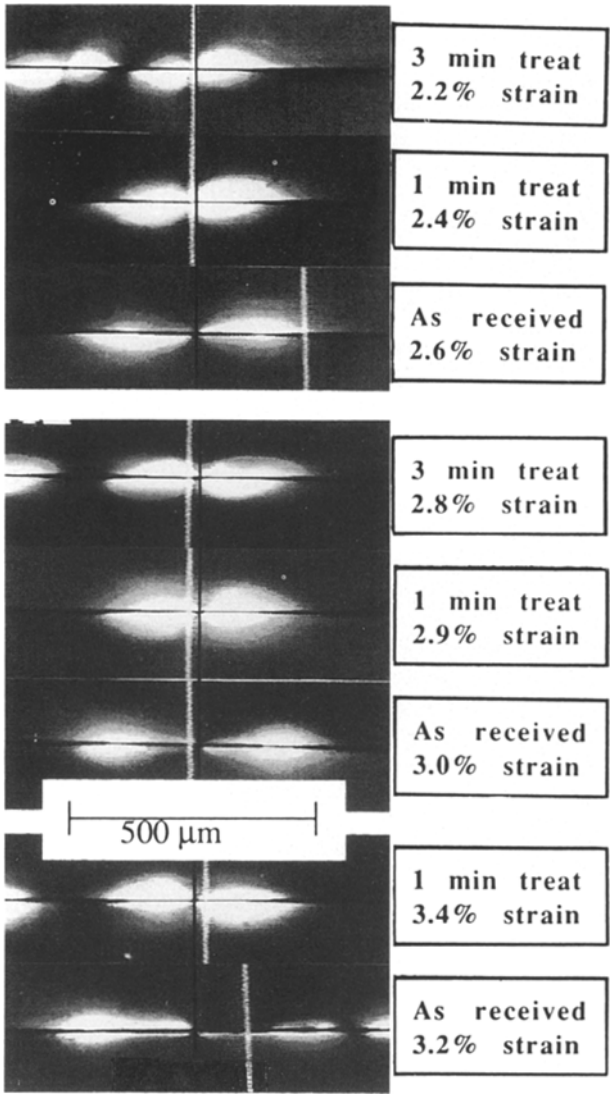

Figure 9 Typical photoelastic patterns in J2 for as-received fibres, and fibres treated for 1 and 3 min at several strain levels.

The texture of the fibre surface changes with treatment time. The surface of the bare as-received fibre is striated, but is otherwise very smooth. As the fibre is treated the surface is etched unevenly, leaving behind protrusions that increase in density. The surface of the as-received fibres that are pulled from polycarbonate is also striated; however, the striations are deeper, and the surface between the striations is slightly rough. The interpretation is that during fibre pull-out, the interphase failed in the fibre portion of the interphase. The surface of the 1 min treated fibre has a few striations, but most of the surface is covered with extrusions and protrusions that are more consistent and larger than the protrusions observed on the bare fibre; they are therefore interpreted to be polycarbonate fragments remaining on the fibre surface. The 3 min treated fibre differs from its bare counterpart in the size of the surface features; the larger protrusions are polycarbonate on the surface. When the fibre treated for 1 min was pulled from the matrix, the interphase crack meandered through both the matrix and the fibre, and when the fibre treated for 3 min was removed from the matrix, the interphase failed in the matrix region of the interphase. The fibre pulled from J2 experiences almost the same sequence of events as a function of treatment time. The surface of the as-received fibre pulled from J2 looks more like a bare filament than the surface of the as-received fibre pulled from the polycarbonate. The interphase failure may therefore have occurred at the fibre–matrix interface. The treated fibres have remnants of matrix on the fibre surface, indicating that the interphase crack occurred primarily in the matrix region of the interphase.

Further evidence that the fibre surface of the treated fibres pulled from the matrix is covered with matrix is shown in Fig. 11. This shows the very edge of the matrix and the beginning of the fibre pull-out. The matrix can be seen pulling off the fibre and leaving remnants behind.

4. Discussion

The discussion of these data has many facets. Therefore the discussion is broken into several sections. The fibre surface morphology and fibre surface energy are discussed in terms of how the observed behaviour might contribute to strengthening the interphase. The micromechanics of the load transfer from the matrix to the fibre are discussed next. The average ISS is correlated with the fibre strength, surface energy, and surface morphology both before and after moulding; a comparison is drawn between the behaviour of AU4 in polycarbonate and that in J2.

4.1. Surface morphology and surface energy

The change in fibre surface roughness and fibre surface energy with treatment time is reported in Fig. 5a. The surface roughness is seen to reach a maximum after 3 min of treatment, and then decrease; the surface energy increases dramatically after 1 min of treatment (the increase is mostly due to an increase in the polar component) and then levels off.

The fibre surface is roughened during treatment because material is etched unevenly from the surface, resulting in surface voids (an increase in roughness). The decrease in roughness after 4 min of treatment occurs because as etching continues, the number of voids increases until the voids begin to coalesce; this coalescence creates a decrease in the density of protrusions, and thus a decrease in roughness.

An increase in fibre surface roughness could improve the load transfer from the matrix to the fibre in two ways. Etching of the fibre surface may remove weak boundary layers which may increase the shear strength of the interphase, and thus the ability of the interphase to transfer load [26]. The etching process employed here removes up to 3% of the diameter, which is about 200 nm after 5 min of treatment. A typical crystallite measures 2–5 nm; therefore if there is a weak boundary layer, the fibre treatment may remove all or part of it.

The second mechanism for increasing the average ISS could be an improved micromechanical interlocking of the fibre and the matrix [17, 27]. A rough surface allows more interpenetration of the two materials. However, the improved mechanical coupling

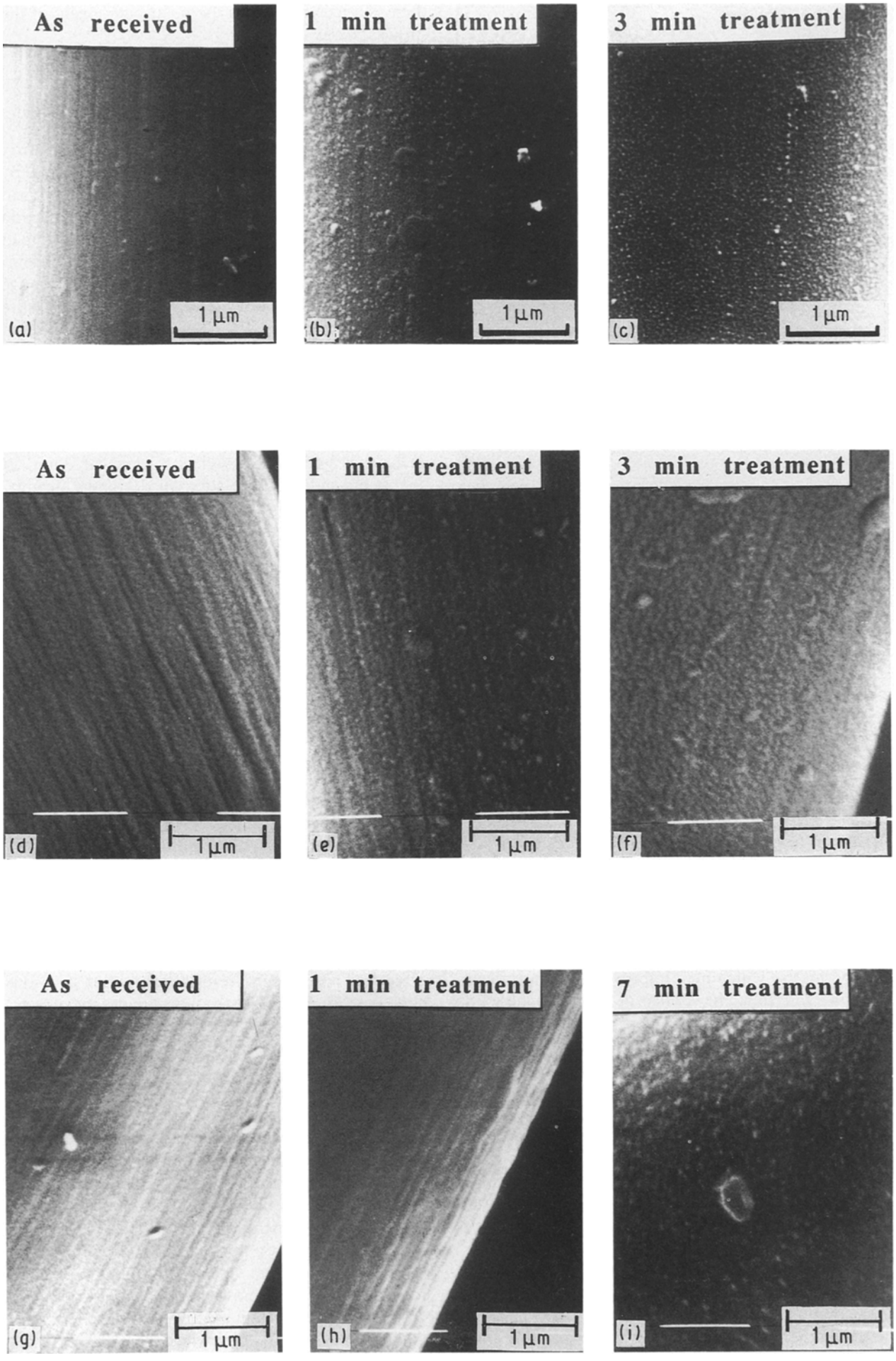

Figure 10 SEM fractographs showing the difference between (a–c) unmoulded AU4 fibres, (d–f) fibres pulled out of polycarbonate, and (g–i) fibres pulled out of J2 at various treatment times.

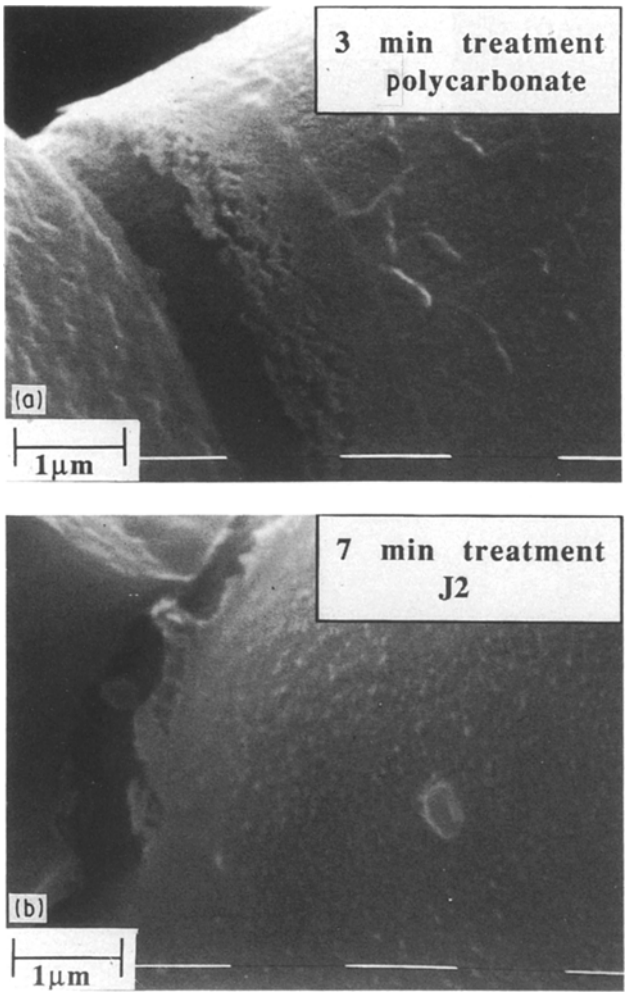

Figure 11 SEM fractographs depicting the fibre pulling out from the two matrices: (a) polycarbonate, (b) J2.

must be accompanied by the ability of the matrix to wet the fibre (physical coupling) [5]. Fortunately, as the treatment etches the fibre surface it increases the polar component of the surface energy which improves the matrix wetting of the fibre.

A higher surface energy can also be beneficial because it can improve the chemical bonding of the fibre and the matrix which may improve interphase shear strength, and thus the ability of the interphase to transfer load.

Consider the surface energy data in more detail (Fig. 7). The surface energy of the fibre reaches a plateau at about 70 dyn cm^{-1} (mN m^{-1}) after 3 min of treatment. After 1 min of treatment, the polar component reaches 40 dyn cm^{-1}, and does not increase further, but the dispersive component increases continuously. The surface energy of water is 72 dyn cm^{-1}, and its polar component is 49 dyn cm^{-1}. Unfortunately, the sensitivity of the Wilhelmy test is limited by the surface energy of the liquid used. If a solid's surface energy, polar component, or dispersive component is equal to that component of the liquid, any increase in that component of the surface energy will not be detected. Therefore, the surface energy of the fibre may continue to increase after 3 min of treatment, but it would not be detected. However, the polar component reached a plateau below 49 dyn cm^{-1}, suggesting that there is a true plateau in the polar component of the surface energy.

4.2. Interphase micromechanics

The micromechanics of load transfer from the matrix to the fibre through the interphase is affected by chemical bonding, chemical coupling, mechanical coupling and physical coupling [5]. This section attempts to determine which mechanisms of load transfer are acting in the AU4–PC and AU4–J2 composite systems. To begin the discussion, the average ISS is correlated with the fibre surface roughness, fibre surface energy and fibre strength as a function of treatment time for both composite systems (Fig. 5). The figure can be summarized as follows: the average ISS for AU4–PC peaks between 3 and 4 min, while the average ISS for AU4–J2 reaches a plateau after 1 min of treatment; the fibre surface energy reaches a plateau after 2 to 3 min; the roughness peaks at 3 min of treatment; and the fibre strength decreases steadily. The load transfer behaviour in AU4–PC will be discussed first.

The above summary emphasizes the correlation between the average ISS behaviour in AU4–PC and the surface roughness; both reach a peak at about 3 min of treatment time. This correlation suggests that the improvement in the mechanism of load transfer is influenced by micromechanical interlocking more than by physical coupling, chemical coupling or chemical bonding. However, the surface energy does have a role; if the matrix cannot wet the fibres, the increased roughness will not result in improved mechanical interlocking because the matrix will not be able to fill in the holes. Therefore the polar component of the fibre surface energy must be high enough for the matrix to be able to wet the fibre.

The improved mechanical interlocking in AU4–PC can also be observed in SEM micrographs of fibres pulled from the matrix (Fig. 10). As the treatment time is increased from 1 to 3 min, there is an increased participation of the matrix. As mentioned earlier, the as-received fibres pulled from PC exhibit the striations of the bare fibre, but the striations are deeper suggesting that the interphase failure occurred some distance into the fibre. The treated fibres pulled from PC have polycarbonate on their surface, suggesting that the matrix interacted more strongly with the fibre, resulting in an interphase failure some distance into the matrix. At intermediate treatment times (1 min), the interphase failure meandered between the matrix and the fibre. The appearance of striations on the surface of the 1 min treated fibre as well as some polycarbonate support this conclusion.

These data alone do not rule out the hypothesis by Drzal *et al.* [26] that improved average ISS after etching is due to the removal of weak boundary layers. However, the decrease in average ISS and the surface roughness after 4 min implies that the roughness is an important parameter. It may be that both mechanisms play a role in improving the load transfer from the matrix to the fibre.

In AU4–J2 the average ISS correlates more closely with the surface energy than the surface roughness. Both the surface energy and the average ISS reach a plateau after 1 to 2 min of treatment time. This suggests that the load transfer is due to physical coupling or chemical bonding. However, after 1 to 2 min of treatment time, when the fibre fails in the fragmentation test, a crack extends into the matrix perpendicular to the fibre at the fibre break. This crack relieves the strain in the fibre to an unknown level lower than the one used for calculating the average ISS. This means that the values reported overestimate the values for the average ISS in J2 specimens containing treated fibres. The mere presence of a transverse matrix crack in these specimens, however, indicates that these interphases are actually stronger in shear than the interphase in the composites with as-received fibres. If continued surface treatment had weakened the resulting fibre–matrix interphase sufficiently, then failure would again have occurred along the interphase. When the interphase is forced to fail by fibre pull-out, SEM micrographs indicate that the increased participation of the matrix observed in PC is observed in J2. This indicates that the average ISS would follow a trend similar to that in polycarbonate. Therefore the mechanism for improved average ISS in the J2 composites is also due to improved micromechanical interlocking, a mechanism which suggests that the properties of the J2 matrix strongly influence the load transfer behaviour of the interphase. On the basis of this rationale, the higher average ISS in J2 composites versus PC composites could be due to the differences in the matrix properties.

Fig. 3 shows schematically the interphase crack that develops after fibre failure, and during subsequent loading. Γ and β represent the growth of the crack into the matrix and along the fibre, respectively. Polycarbonate is a tough, strong matrix such that $\Gamma \approx 0$, and β grows during the fragmentation test. The photoelastic patterns (Fig. 7) provide evidence for this. As the sample is loaded, the stress transfer zone moves along the fibre. J2 is a weaker matrix; Γ grows for fibres treated more than 2 min while β is constant. For as-received fibres in J2, Γ is small and β grows during the test. The photoelastic patterns again provide good evidence of this (Fig. 8). The length of the stress transfer zone for treated fibres is constant with applied strain, implying that β is constant; a crack can be seen perpendicular to the fibre extending into the matrix. This effect of the matrix has been observed in other systems [28]; in more flexible, weaker epoxies, a matrix crack perpendicular to the fibre developed during a fragmentation test; in stronger epoxies, failure occurred along the interphase.

There is evidence in graphite–epoxy systems which suggests that the toughness and mode of failure in polycarbonate and J2 composites would differ significantly. For example, Drzal [2] examined the differences in fracture toughness perpendicular and parallel to the fibre direction in graphite–epoxy composites. He found that the highest interphase shear stress that yielded a crack growing perpendicular to the fibre in monofilament composites resulted in a brittle planar failure, while monofilament composites in which the interphase failed along the fibre resulted in energy being expended into debonding and fibre pull-out, yielding a tougher material with a rough failure surface. The best off-axis properties were found in the composite with the highest ISS.

5. Conclusions

Studies of interphase behaviour in graphite–PC and graphite–J2 systems, in which the interphase had been systematically varied, lead to the following conclusions.

1. The surface roughness and surface energy of the graphite fibre both varied with etching. The improvement in load transfer from the matrix to the fibre in AU4–PC composites correlated strongly with the surface roughness, indicating that the improvement in average ISS is mainly a result of improved micromechanical interlocking. The improvement in load transfer in the AU4–J2 composites was difficult to determine due to cracks forming perpendicular to the interphase. Evidence from SEM micrographs indicate that any improvement in the interphase shear strength is also due to improved micromechanical locking.

2. The interphase failure path in AU4–polycarbonate composites was always parallel to the fibre while in AU4–J2 composites, if the interphase was strong, failure occurred perpendicular to the fibre into the matrix. This behaviour suggests that the optimal interphase behaviour depends not only on the fibre surface, but also on the matrix properties.

Acknowledgements

The work was supported jointly by the E. I. Du Pont de Nemours and Co., Inc., and by the University of Pennsylvania under the auspices of the Laboratory for Research on the Structure of Matter (Composites interface thrust). The work was further promoted by the generous advice and assistance of A. L. Radin and D. Ricketts at the University of Pennsylvania, and L. Peterson and B. Campbell at E. I. Du Pont de Nemours and Co Inc. Discussions with Z. Hashin were very helpful.

References

1. R. C.TENNYSON, T. A. WATERHOUSE, S. NEWMAN and M. T. TAKEMORI, *Polym. Compos.* **6** (1982) 437.
2. L. T. DRZAL, *Adv. Polym. Sci.* **75** (1986) 1.
3. A. N. NETRAVALI, R. B. HENSTENBERG, S. L. PHOENIX and P. SCHWARTZ, *Polym. Compos.* **10** (1989) 226.
4. L. DiLANDRO, A. T. DiBENEDETTO and J. GROEGER, *ibid.* **9** (1988) 209.
5. P. EHRBURGER and J. B. DONNET, *Phil. Trans. R. Soc. Lond.* **A294** (1980) 495.
6. D. H. KAELBLE, *J. Adhesion* **5** (1973) 245.
7. W. GUTOWSKI, *ibid.*, **23** (1987) 187.
8. J. L. KARDOS, "Molecular Characterization of Composite Interfaces" (Plenum, 1985).
9. N. SATO, T. KURAUCHI, S. SATO and O. KAMIGAITO, *J. Mater. Sci. Lett.* **2** (1983) 188.

10. J. NAIRN and P. ZOLLER, *J. Mater. Sci.* **20** (1985) 355.
11. F. J. McGARRY and M. FUJIWARA, in Proceedings of 23rd Annual Technical Conference, Reinforced Plastics Division (SPI) (1968).
12. W. D. BASCOM and R. M. JENSEN, *J. Adhesion* **19** (1986) 219.
13. C. GALIOTIS, Private Communication (1990).
14. A. T. DiBENEDETTO, L. NICOLAIS, L. AMBROSIO and J. GROEGER, in Proceedings of 1st International Conference on Composite Interfaces (ICCI-I), Cleveland, Ohio, 1986, edited by H. Ishida and J. L. Koenig (Elsevier Science, NY, 1986) p. 47.
15. L. DiLANDRO, A. T. DiBENEDETTO and J. GROEGER, *Polym. Compos.* **9** (1988) 209.
16. M.NARKIS, E. J. H. CHEN and R. B. PIPES, *ibid.* **9** (1988) 245.
17. J. C. FIGUEROA, L. S. SCHADLER and C. LAIRD, in Proceedings of the Materials Research Society, November 1989, Vol. 170, edited by C. G. Pantano and E. J. H. Chen (Materials Research Society, Pittsburgh, PA, 1989) p. 65.
18. L. S. SCHADLER, J. C. FIGUEROA and C. LAIRD, *ibid.* p. 345.
19. M. NARKIS, S. CHAOUAT-SIBONY, L. NICOLAIS, A. APICELLA and J. P. BELL, *Polym. Commun.* **26** (1985) 339.
20. B. MILLER and R. A. YOUNG, *J. Textile Res.* **45** (1975) 359.
21. S. WU, "Polymer Interface and Adhesion" (Dekker, New York, 1982).
22. H. J. BUSSCHER, A. W. J. Van PELT, P. De BOER, H. P. JONG and J. ARENDS, *Colloids & Surfaces* **9** (1984) 319.
23. A. KELLY and W. R. TYSON, *J. Mech. Phys. Solids* **13** (1965) 329.
24. L. S. SCHADLER, N. MELANITIS, C. GALIOTIS, J. C. FIGEUROA and C. LAIRD, *J. Mater. Sci.* in press.
25. L. S. SCHADLER, J. C. FIGUEROA and C. LAIRD, in Proceedings of Advanced Materials Conference II, March 1989, edited by F. W. Smith (Advanced Materials Institute, Denver, CO, 1989) p. 638.
26. L. T. DRZAL, M. J. RICH, M. F. KOENIG and P. F. LLOYD, *J. Adhesion* **16** (1983) 133.
27. U. GAUR and T. DAVIDSON, in Proceedings of the Materials Research Society, November 1989, Vol. 170, edited by C. G. Pantano and E. J. H. Chen (Materials Research Society, Pittsburgh, PA, 1989) p. 309.
28. E. T. M. ASLOUN, N. NARDIN and J. SCHULTZ, *J. Mater. Sci.* **24** (1989) 1835.

Received 16 January
and accepted 17 May 1991